

Studies on the binding of nevadensin to human serum albumin by molecular spectroscopy and modeling

Daojin Li, Jingfeng Zhu, Jing Jin ^{*}, Xiaojun Yao

Department of Chemistry, Lanzhou University, Lanzhou 730000, China

Received 24 September 2006; received in revised form 24 December 2006; accepted 8 January 2007

Available online 21 January 2007

Abstract

The binding of nevadensin to human serum albumin (HSA) in aqueous solution was investigated for the first time by molecular spectroscopy and modeling at pH 7.4. Spectrophotometric observations are rationalized in terms of a static quenching process and binding constant (K_a , K_b) and the number of binding sites ($n \approx 1$) were evaluated by fluorescence quenching methods. Thermodynamic data showed that nevadensin was included in the hydrophobic cavity of HSA mainly via hydrophobic interactions. The value of 3.09 nm for the distance r between the donor (HSA) and acceptor (nevadensin) was derived from the fluorescence resonance energy transfer. Spectrophotometric techniques were also applied to investigate the structural information of HSA molecules on the binding of nevadensin and the results showed that the binding of nevadensin to HSA did not change significantly molecular conformation of HSA in our experimental conditions. Furthermore, the study of molecular modeling also indicated that nevadensin could strongly bind to the site I (sub-domain IIA) of HSA mainly by a hydrophobic interaction and there are hydrogen bond interactions between nevadensin and the residues Arg-218, Arg-222, Lys-195, and Asp-451. As compared to the other flavonoids, the flavonoids containing methoxy groups which are in aromatic rings can bind to HSA with higher affinity.

© 2007 Elsevier B.V. All rights reserved.

Keywords: Nevadensin; Human serum albumin; Fluorescence quenching; Circular dichroism (CD); Molecular modeling

1. Introduction

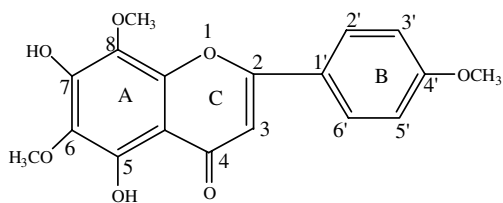
Human serum albumin (HSA) as the most abundant carrier protein plays an important role in the transport and disposition of many endogenous and exogenous substances such as metabolites, drugs, and other biologically active compounds present in blood [1]. And the investigation of the interaction of HSA with drugs contributes to understand disposition, transportation, metabolism and efficacy of drugs, which are correlated with their affinities toward HSA. Therefore, it is of great importance to study the binding of such small molecules to HSA.

The flavonoids are made up of an important group of naturally occurring bioactive polyphenolics, ubiquitous in plants of higher genera. The basic structure of flavonoids

(see [Scheme 1](#)) is usually characterized by three rings (A, B, and C) and there are two aromatic rings (A and B), which are joined by a three-carbon linked γ -pyrone ring (C), forming a $C_6-C_3-C_6$ skeleton unit where side group is usually hydroxyl, methoxyl or glycosyl.

As early as 1936, since Rusznyak and Szent-Gyorgyi [2] first recognized the therapeutically beneficial role of dietary flavonoids, there is growing evidence for flavonoids with a wide range of therapeutic activities of high potency and low systemic toxicity [3] such as against cancers, tumors, AIDS, and inflammation, etc. Recent interests on flavonoids have largely focused on their biological and relevant therapeutic applications. It has even been confirmed that HSA can play a decisive role in the transport and disposition of flavonoids [4]. A number of biochemical and molecular biological investigations have showed that proteins are frequently the “targets” for therapeutically active flavonoids of both natural and synthetic origin [5], so it is necessary to study the interaction between flavonoids and protein in order

^{*} Corresponding author. Tel.: +86 931 8912293; fax: +86 931 8625657.
E-mail addresses: jinjing@lzu.edu.cn, lni615@126.com (J. Jin).



Scheme 1. The chemical structure of nevodensin.

to understand the mechanism of drug action at a molecular level. However, until now, very little was known about the specific mode of interactions of these compounds with their respective target proteins at the molecular level. Moreover, although there have ever been a large amount of studies on the interaction of flavonoids with HSA [6–17], until today, the binding of flavonoids containing several methoxyl groups ($-\text{OCH}_3$) to HSA has seldom been reported. The interaction of nevodensin with HSA has not been carried out. Nevadensin (Scheme 1) is one of the flavonoids widely used in traditional Chinese medicine for the treatment of lymph node tuberculosis, cough with tachypnoea and rheumatic pains [18,19] and is widely on the distribution in plants of *Lysionotus pauciflorus* Maxim, which is widespread in southern China.

In this work, we have performed for the first time extended studies on the interaction of HSA with nevodensin in aqueous solutions at three temperatures under physiological conditions utilizing fluorescence method in combination with synchronous fluorescence and CD technique. Furthermore, the molecular modeling was studied with Sybyl 6.9 package on SGI FUEL workstation.

2. Materials and methods

2.1. Materials and preparation of solutions

Human serum albumin (HSA, fatty acid-free <0.05%), purchased from Sino-American Biotechnology Company, was used without further purification. Nevadensin was of analytical grade, and purchased from the National Institute for Control of Pharmaceutical and Bioproducts, China. Tris(hydroxymethyl-aminomethane) was of biochemical grade and was purchased from Shanghai Chemical Reagent Head Factory (Shanghai, China). NaCl (analytical grade, 1 mol/L) solution was used to maintain the ion strength at 0.1. Tris-HCl buffer solution (0.05 mol/L Tris, 0.1 mol/L NaCl) was used to keep the pH of the solution at 7.40. HSA stock solution of 1.5×10^{-5} mol/L was prepared with the Tris-HCl buffer solution and kept in the dark at 4 °C. The stock solution (5×10^{-4} mol/L) of nevodensin was prepared by dissolving appropriate amount of nevodensin in 50 ml anhydrous methanol. The working solution (1.0×10^{-4} mol/L) was obtained by appropriate dilution of the stock solution with methanol. All other reagents were of analytical grade and doubly distilled water was used throughout all the experiments. The concentration of HSA was determined spectrophotometrically on a Shimadzu

UV-260 UV-vis spectrophotometer using ϵ_{280} (HSA) = 36,500/M/cm [12].

2.2. Apparatus and methods

Fluorescence measurements were performed on an LS-55 spectrofluorophotometer (Perkin-Elmer, America) following an excitation at 280 nm. The fluorescence emission spectra were recorded in the wavelength of 290–500 nm. Both excitation and emission bandwidths were adjusted at 10 nm. The synchronous fluorescence spectra were obtained by scanning simultaneously the excitation and emission monochromator. The wavelength interval ($\Delta\lambda$) is fixed individually at 15 and 60 nm, at which the spectrum only shows the spectroscopic behavior of Tyr and Trp residues of HSA, respectively. The quantitative analysis of the interaction between HSA and nevodensin was performed by a fluorometric titration as follows: 3 mL of a 1.5×10^{-6} mol/L solution of HSA was titrated by successive addition of nevodensin solution to reach a final concentration of 3×10^{-6} mol/L nevodensin.

Circular dichroism measurements were run on an Olis DSM 1000 automatic recording photospectrometer using a cell with 1 mm optical length at 296 K, with three scans averaged for each CD spectra at room temperature (296 K). CD determinations of pure HSA and HSA-nevodensin mixtures were carried out using the buffer solutions of nevodensin at a corresponding concentration as the reference. The results are expressed as ellipticity (mdeg), which was obtained in mdeg directly from the instrument.

The potential of the 3D structure of HSA was assigned according to the Amber 4.0 force field with Kollman-all-atom charges. The initial structures of all the molecules were generated by molecular modeling software Sybyl 6.9 [20]. The geometries of this drug were subsequently optimized using the Tripos force field with Gasteiger–Marsili charges. FlexX program was applied to calculate the possible conformation of the drug that binds to the protein. The crystal structure of HSA in complex with R-warfarin was taken from the Brookhaven Protein Data Bank (entry codes 1h9z). The PDB file contains a co-crystal with a small ligand (R-warfarin) in the active site. This ligand was extracted and used as a reference structure (a fixed conformation docked into the active site of the HSA). FlexX program used the reference structure for the active site determination – by default, any residue in the protein within 6.5 Å of the reference structure was considered part of the active site. FlexX program also did an RMS comparison between the reference structure and final docked structure of nevodensin as an indication of accuracy. The receptor descriptor file (rdf) lies at the heart of FlexX. It contains the information about the protein, its amino acids, the active site, non-amino acid residues, and specific torsion angles. Sybyl interface to FlexX created a default-rdf file. At last, FlexX program was used to build the interaction modes between the nevodensin and HSA. Nevadensin was docked to HSA by FlexX and then it

revealed hydrogen bonds between nevadensin and some residues of HSA. All calculations were all performed through SGI FUEL workstations.

3. Results and discussion

3.1. Analysis of fluorescence quenching of HSA by nevadensin

Fluorescence of HSA originates from tryptophan (Trp), tyrosine (Tyr) and phenylalanine (Phe) residues. Actually, the intrinsic fluorescence of HSA is mainly contributed by the Trp residue alone, because the Phe residue has a very low quantum yield and the fluorescence of Tyr is almost totally quenched when it is ionized or near by an amino group, a carboxyl group or a Trp [21]. That is, the change of intrinsic fluorescence intensity of HSA is mainly that of Trp residue when small molecule substances are bound to HSA.

The ultimate percentages of methanol in all solutions were below 3% (v/v). Because nevadensin was prepared in methanol, the quenching effect of methanol, and the effect of methanol on HSA conformation were then evaluated. The results showed that the effect of methanol on the nevadensin interaction with HSA could be negligible in the amount used in our experiment. Fig. 1 showed the fluorescence emission spectra of HSA with various amount of nevadensin following an excitation at 280 nm. It could be seen that the fluorescence intensity of HSA dropped regularly with the increase in nevadensin concentration, indicating that nevadensin can bind to the HSA, which was discussed further later.

3.2. Fluorescence quenching mechanism of HSA by nevadensin

A quenching process can be usually induced by a collisional process or a formation of a complex between

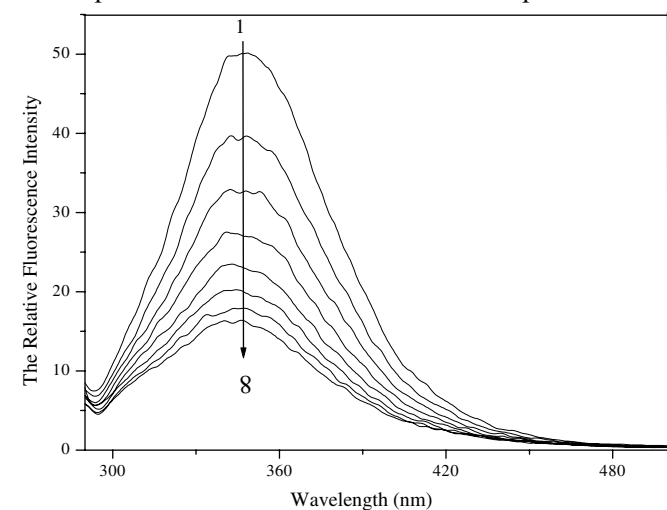


Fig. 1. The fluorescence spectra of the nevadensin-HSA system. [HSA] = 1.5×10^{-6} mol/L, [nevadensin] = 0, 3, 6, 9, 12, 15, 18, 21 ($\times 10^{-7}$ mol/L) (1 \rightarrow 8); $T = 296$ K, pH 7.40; $\lambda_{\text{ex}} = 280$ nm.

quencher and fluorophore. The former is referred to as a dynamic quenching mechanism and the latter a static quenching mechanism. Both mechanisms can be distinguished from each other by the differences in temperature-dependent behavior. It is well known that dynamic quenching mainly depends upon diffusion. Since higher temperatures can result in larger diffusion coefficients, the bimolecular quenching constants are expected to increase with increasing temperature. In contrast, a static quenching process will lead to a decrease in the quenching rate constant with raising temperature.

In order to confirm the quenching mechanism, the fluorescence quenching was analyzed according to the well-known Stern–Volmer equation [22]:

$$\frac{F_0}{F} = 1 + k_q \tau_0 [Q] = 1 + K_{SV} [Q] \quad (1)$$

where, F_0 and F represent the steady-state fluorescence intensities in the absence and in the presence of quencher, respectively, $[Q]$ is the concentration of quencher. k_q is the quenching rate constant of biomolecule, τ_0 is the average life-time of biomolecule without the quencher and its value is 5 ns [13] and K_{SV} is the Stern–Volmer dynamic quenching constant, which was determined by linear regression of a plot of F_0/F against $[Q]$. The solid lines in Fig. 2 show the lines of best fit of the experimental data to the Stern–Volmer equation. The values for K_{SV} , k_q , R , and linear regression equation at different temperatures are presented in Table 1. The results in Table 1 shows K_{SV} is inversely correlated with temperature, which suggests that the fluorescence quenching process may be mainly controlled by a static quenching mechanism rather than a dynamic quenching mechanism. Moreover, values for k_q (Table 1) are four orders of magnitude greater than the maximum diffusion collision quenching rate constant

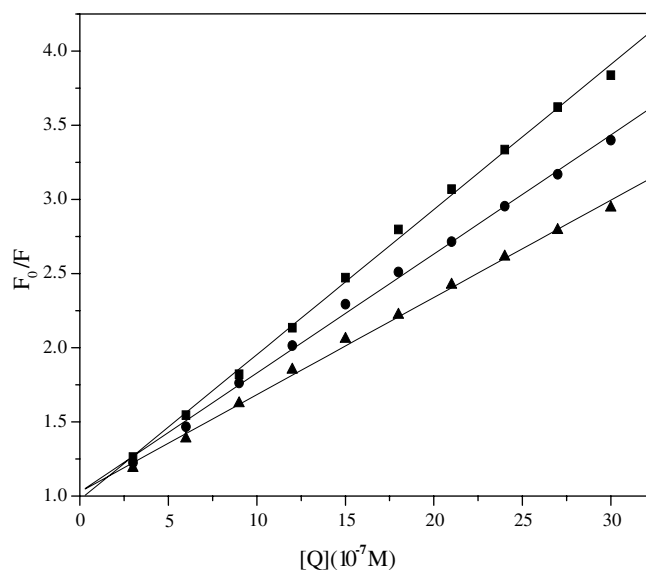


Fig. 2. The Stern–Volmer plots of HSA quenched by nevadensin : ■, 296 K; ●, 306 K; ▲, 318 K. [HSA] = 1.5 μ M, $\lambda_{\text{ex}} = 280$ nm, pH = 7.40.

Table 1
Stern–Volmer quenching constants of the system of nevadensin–HSA at different temperatures

pH	T (K)	K_{SV} ($\times 10^5$ L/mol)	k_q ($\times 10^{14}$ L/mol/s)	R linear regression equation
7.4	296	9.781	1.956	$F_0/F = 0.976 + 9.781 \times 10^5 [Q]$
	306	8.031	1.606	$F_0/F = 1.026 + 8.031 \times 10^5 [Q]$
	318	6.558	1.312	$F_0/F = 1.028 + 6.558 \times 10^5 [Q]$

R is the correlation coefficient.

(2.0×10^{10} L/mol/s) of a variety of quenchers with biopolymer [23]. This result indicates again that the quenching is not caused by dynamic collision but from the formation of a complex.

3.3. Determinations of binding constants and the number of binding sites

For the static quenching process, the quenching data were analyzed according to the modified Stern–Volmer equation [24]:

$$\frac{F_0}{\Delta F} = \frac{1}{fK_a} \frac{1}{[Q]} + \frac{1}{f} \quad (2)$$

In the present case, F_0 and ΔF are the relative fluorescence intensity without quencher and the difference in fluorescence intensity of protein in the absence and presence of quencher, respectively. K_a is the effective quenching constant for the accessible fluorophores, here it is binding constant and $[Q]$ is the quencher concentration; f is the fractional maximum fluorescence intensity of protein summed up, and the plot of $F_0/\Delta F$ versus $[Q]^{-1}$ is linear with slope equalling to the value of $(fK_a)^{-1}$. The value $1/f$ is fixed on the ordinate. The association constant K_a is a quotient of an ordinate $1/f$ and slope $(fK_a)^{-1}$.

Fig. 3 shows the modified Stern–Volmer plots for the system of nevadensin–HSA at different temperatures. The

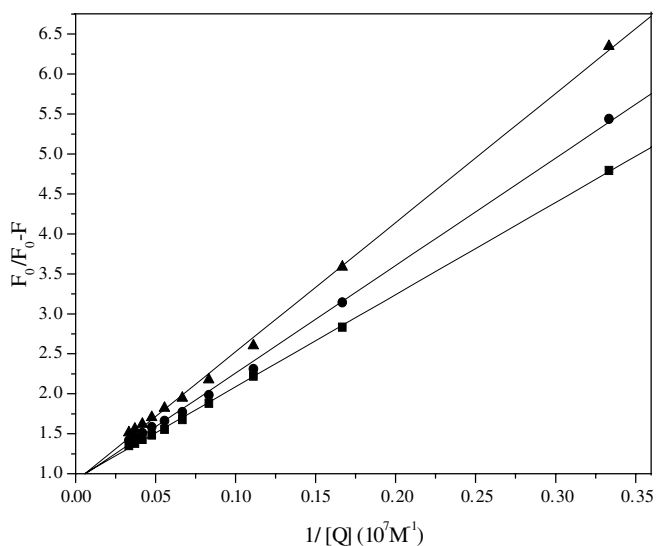


Fig. 3. The modified Stern–Volmer plots for the nevadensin–HSA system at pH 7.40: ■, 296 K; ●, 306 K; ▲, 318 K. $[HSA] = 1.5 \mu M$, $\lambda_{ex} = 280$ nm.

corresponding results at different temperatures are listed in Table 2. It could be observed that values of K_a decreased with the temperature rising, which was in accordance with K_{SV} 's dependence on temperature as mentioned above. This result indicates that the interaction between nevadensin and HSA was weakened when the temperature rose.

When small molecules bind independently to a set of equivalent sites on a macromolecule, the equilibrium between free and bound molecules is given by the following equation [11].

$$\log \frac{(F_0 - F)}{F} = \log K_b + n \log [Q] \quad (3)$$

where, in the present case, K_b is the binding constant, and n is the number of the binding sites per HSA, which can be determined by the ordinate and slope of double logarithm regression curve (Fig. 4) of $\log (F_0 - F)/F$ versus $\log [Q]$ based on the Eq. (3), respectively. The values of K_b and n were evaluated and presented in Table 3. It indicates that nevadensin binds to HSA with high affinity and there is about one binding site on the protein. It also shows that the values of K_b and n decreased with the temperature increasing, which may imply that a unstable complex was formed in the binding reaction. The complex would possibly be partly dissociated when the temperature increases, therefore, the values of K_b and n decreased with the temperature rising, which also agreed with the trend of K_{SV} and K_a , as mentioned above.

3.4. Binding mode

Essentially, there are four types of non-covalent interaction existing in ligand binding to proteins. These are hydrogen bonds, van der Waals forces, hydrophobic bonds and electrostatic interactions. The thermodynamic parameters of binding reaction are the main evidence for confirming acting forces. Therefore, the thermodynamic parameters dependent on temperatures were analyzed in order to characterize the acting forces between drug and HSA. If the enthalpy change (ΔH^0) changes little in the temperature range studied, thermodynamic parameters (ΔH^0 and ΔS^0) were calculated from the Vant Hoff plot (Fig. 5) based on Eq. 4 and listed in Table 2. The free energy change ΔG^0 of the binding reaction at different temperature is estimated from the Eq. 5 and displayed in Table 2.

$$\ln K_a = -\frac{\Delta H^0}{RT} + \frac{\Delta S^0}{R} \quad (4)$$

Table 2
Modified Stern–Volmer binding constants K_a and relative thermodynamic parameters of the system of nevadensin–HAS

pH	T (K)	K_a ($\times 10^5$ L/mol)	R^a	ΔH^0 (kJ/mol)	ΔG^0 (kJ/mol)	ΔS^0 (J/mol/K)	R^b
7.4	296	8.114	0.99983	–13.050	–33.484	69.034	0.99999
	306	6.815	0.99917		–34.174		
	318	5.622	0.99924		–35.003		

R^a and R^b is the correlation coefficient for the K_a values and for thermodynamic parameters, respectively.

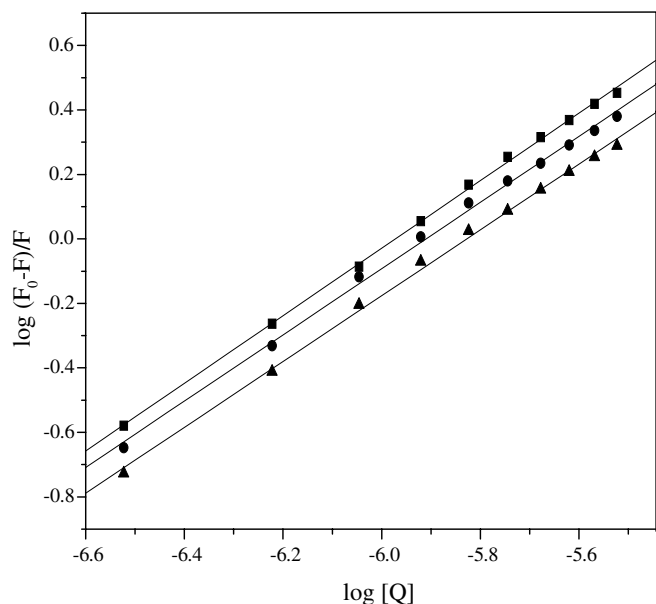


Fig. 4. Plots of $\log(F_0 - F)/F$ versus $\log[Q]$ for the nevadensin–HSA system at pH 7.40: ■, 296 K; ●, 306 K; ▲, 318 K. [HSA] = 1.5 μ M, λ_{ex} = 280 nm.

Table 3
Binding constants K_b and binding sites n at different temperatures

pH	T (K)	K_b ($\times 10^6$ L/mol)	n	R
7.4	296	1.807	1.048	0.99955
	306	1.173	1.027	0.99873
	318	0.889	1.021	0.99871

R is the correlation coefficient.

$$\Delta G^0 = \Delta H^0 - T\Delta S^0 \quad (5)$$

where K_a is the modified Stern–Volmer quenching constants at absolute temperature T and R is gas constant.

From Table 2, it can be seen that ΔH^0 is –13.050 kJ/mol, whereas ΔS^0 is 69.034 J/mol K, which indicates that the binding process is exothermic reaction accompanied by a positive ΔS^0 value. The negative value for ΔG^0 indicates the spontaneity of the binding of nevadensin with HSA. From the point of view of water structure, for a drug–protein interaction, a positive ΔS^0 value is frequently regarded as an evidence for a hydrophobic interaction [25] because the water molecules that are arranged in an orderly fashion around the drug and protein acquire a more random config-

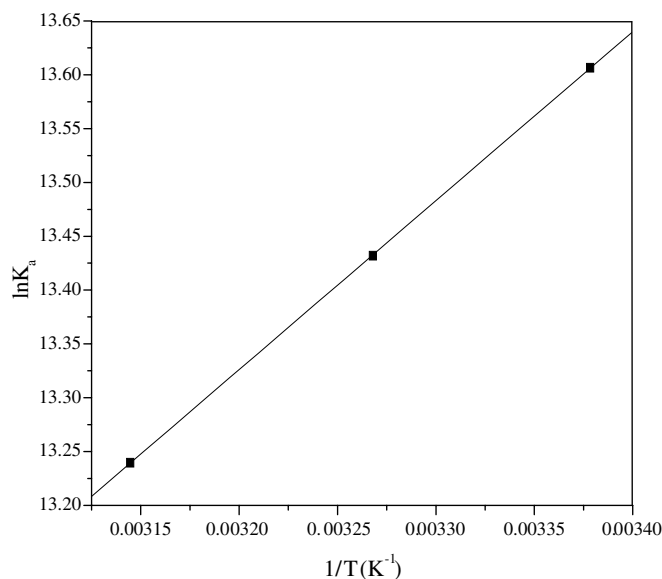


Fig. 5. Vant Hoff plot, [HSA] = 1.5 μ M, pH 7.4.

uration. The negative ΔH^0 value (-13.050 kJ/mol $^{-1}$) observed cannot be mainly attributed to electrostatic interactions since for electrostatic interactions ΔH^0 is very small, almost zero [26,27]. A negative ΔH^0 value will be obtained whenever there exists a hydrogen bonding in the binding reaction [27]. Therefore, it is not possible to account for the thermodynamic parameters according to a single intermolecular force model. Meanwhile, for nevadensin–HSA system, it is found that the main contribution to ΔG^0 value arises from the ΔS^0 rather than from ΔH^0 , so hydrophobic forces most likely play a major role in the binding of nevadensin to HSA, but hydrogen bonding also cannot be excluded.

3.5. Energy transfer between HSA and nevadensin

According to Förster non-radioactive resonance energy transfer theory [28,29], the distances between the protein residue (donor) and the bound drug (acceptor) in HSA could be determined. By Förster's theory, the efficiency of energy transfer (E) is calculated using the equation:

$$E = 1 - \frac{F}{F_0} = \frac{R_0^6}{R_0^6 + r^6} \quad (6)$$

where r is the distance between acceptor (nevadensin) and donor (HSA) and R_0 is the critical distance when the transfer

efficiency is 50%. The value for R_0 is calculated using the equation:

$$R_0^6 = 8.8 \times 10^{-25} k^2 N^{-4} \Phi J \quad (7)$$

In Eq. 8, k^2 is the spatial orientation factor of the dipole, N is the refractive index of medium, Φ the fluorescence quantum yield of donor, and J the spectral overlap between the emission spectrum of donor and the absorption spectrum of acceptor (Fig. 6), which is given by:

$$J = \frac{\int_0^\infty F(\lambda) \varepsilon(\lambda) \lambda^4 d\lambda}{\int_0^\infty F(\lambda) d(\lambda)} \quad (8)$$

where $F(\lambda)$ is the fluorescence intensity of the donor when the wavelength is λ and $\varepsilon(\lambda)$ is the molar absorption coefficient of the acceptor at wavelength λ .

In the present case, it has been reported that $k^2 = 2/3$, $N = 1.366$, and $\Phi = 0.118$ [30,31]. Consequently, we could calculate $J = 6.49 \times 10^{-14} \text{ cm}^3 \text{ L/mol}$, $R_0 = 3.30 \text{ nm}$, $r = 3.09 \text{ nm}$. Obviously, the acceptor–donor distance is less than 8 nm, which implied that the energy transfer from HSA to nevadensin occurred with high possibility.

3.6. Effect of nevadensin on the HSA conformation

3.6.1. Fluorescence and synchronous fluorescence studies

In addition to the proximity of bound nevadensin to Trp residue, fluorescence quenching might result from structural modifications of HSA upon nevadensin binding [32]. Brustein et al [33] considered that maximum emission wavelength (λ_{em}) of the Trp residues is related to the polarity of microenvironment around it. So the changes of maximum emission wavelength of the chromophore will reflect the conformation changes of HSA. It was observed from Fig. 1 that a gradual decrease in the fluorescence intensity

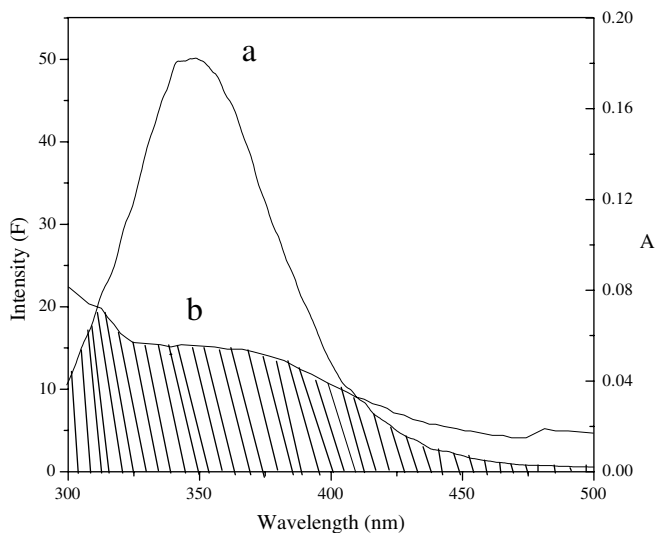


Fig. 6. Overlapping between the fluorescence emission spectrum of HSA (a) ($\lambda_{ex} = 280 \text{ nm}$) and UV absorption spectrum of nevadensin (b). $C_{drug}/C_{HSA} = 1:1$. $T = 296 \text{ K}$.

was caused by quenching but that there was no apparent λ_{em} shift with the increasing nevadensin. This suggests that no change in the conformation of HSA takes place and nevadensin molecules are only located at the close proximity to Trp residue, by which a quenching process occurs.

The observation that the protein conformation might not be changed obviously with the addition of nevadensin was also demonstrated by synchronous fluorescence spectra. As well known, the experiment on synchronous fluorescence of HSA will provide the characteristic information for the Trp residues and Trp residue [34] when the scanning interval $\Delta\lambda$ ($\Delta\lambda = \lambda_{em} - \lambda_{ex}$) was fixed at 15 and 60 nm, respectively. As such, Figs. 7a and b show the synchronous fluorescence spectra of Tyr residues in HSA and those of Trp residues in HSA with various amounts of nevadensin, respectively. It can be seen that the maximum emission wavelength did not shift significant-

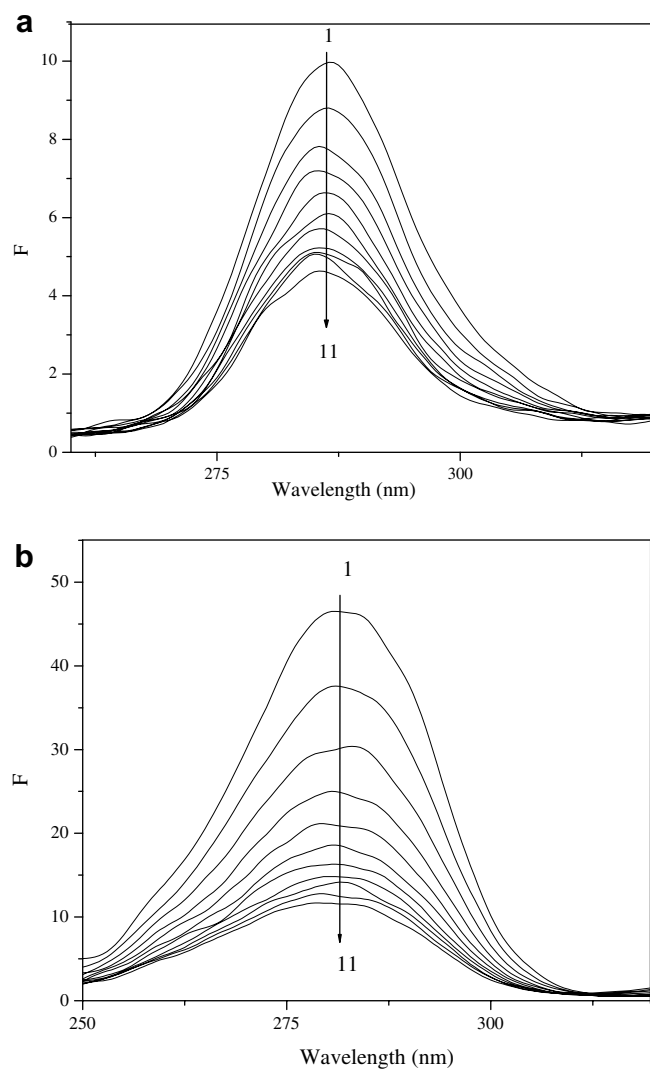


Fig. 7. The synchronous fluorescence spectra of HSA with varying the concentration of nevadensin ((a) $\Delta\lambda = 15 \text{ nm}$ and (b) $\Delta\lambda = 60 \text{ nm}$). $[HSA] = 1.5 \times 10^{-6} \text{ mol/L}$, the concentration of nevadensin (1 \rightarrow 11): 0, 0.3, 0.6, 0.9, 1.2, 1.5, 1.8, 2.1, 2.4, 2.7 and 3.0 ($\times 10^{-6}$) mol/L.

ly, which implied that interaction of nevadensin with HSA does not affect the conformation of the region around the Trp and Try residues.

3.6.2. CD spectra studies

CD is a sensitive technique to monitor the conformational changes in proteins upon an interaction with a ligand. Fig. 8 displays the CD spectra of HSA with various amounts of nevadensin. They exhibit two negative bands at 209 and 222 nm, which is a characteristic of the typical α -helix structure of proteins [7]. The reasonable explanation is that the negative peaks between 208 and 209 nm and 222–223 nm are contributed to $n \rightarrow \pi^*$ transfer for the peptide bond of α -helix [35]. However, it is noticed from Fig. 8 that the addition of nevadensin caused no significant change (slight deviation arising from experiment errors) of the spectrum in either the position or the intensity of the bands in our experiments. This result was in agreement with those obtained from other spectroscopic techniques mentioned above that the interaction with nevadensin had not changed obviously the secondary structure of HSA.

Previous studies on the interaction between BSA and anesthetic chloroform indicated that retention of protein conformation was crucial for ligands binding [32]. This may be the same case as the interaction between HSA and nevadensin. It can be concluded that occupancy of the tryptophan sites by the binding ligands actually could stabilize the native conformation of protein. Frazier et al. [36], Dong et al. [37] and Simon et al. [38] studied the interaction of flavonoids, NR and wine tannin with protein, respectively, and observed that they could bind tightly to protein without modifying its secondary structure, which may agree well with our results reported here.

3.7. Molecule modeling

Crystal structure analysis [39] has revealed that human serum albumin (HSA) consists of a single polypeptide chain of 585 amino acid residues and comprises three structurally homologous domains (I–III): I (residues 1–195), II (196–383), and III (384–585) that assemble to form a heart-shaped molecule. The principal regions of ligand binding sites of HSA are located in hydrophobic cavities in subdomains IIA and IIIA, which are corresponding to site I and site II, respectively and sole tryptophan residue (Trp-214) of HSA is in subdomain IIA. There is a large hydrophobic cavity in subdomain IIA that many drugs can bind. The best score ranked result is showed in Fig. 9. As shown in Fig. 9, nevadensin binds within the subdomain IIA of the protein (The Warfarin Binding Pocket). Nevadensin is located within the binding pocket and the A and C rings are practically coplanar. It can be seen that the glutamic acid residue (Glu292) and tryptophan residue (Trp214) of HSA are in close proximity to the B-ring of nevadensin and 6-OCH₃ in A ring of nevadensin, respectively. These facts suggest the existence of hydrophobic interaction between them. The interaction between nevadensin and HSA is dominated by hydrophobic contacts, but there are also hydrogen interactions between the 5-OH oxygen of nevadensin and Arg218 of HSA, 4-carbonyl oxygen, and Arg222, 8-OCH₃ oxygen and Lys195, as well as 7-OH hydrogen and Asp451.

As compared to other small molecules with the similar structure on non-covalent binding of serum albumin previously reported, the value of the binding constant for nevadensin was relatively large [6–17]. It can be seen from Fig. 9 that this may be because that more atoms are in the plan of heterocyclic ring, thus less steric hindrance would be involved in the binding process. As a result, the binding of nevadensin to HSA became easier relatively. Moreover, three methoxy groups in A and B rings may enhance the binding of the molecule significantly.

4. Conclusions

In the paper, the binding of nevadensin to human serum albumin was investigated by molecular spectroscopy including fluorescence, synchronous fluorescence and circular dichroism (CD) and molecular modeling study under simulative physiological conditions. This study shows that nevadensin binds to HSA with high affinity and quenches the intrinsic fluorescence of HSA efficiently. Binding constants and the number of binding sites (n) are evaluated. The distance (r) between donor and acceptor is obtained according to Förster non-radioactive resonance energy transfer theory. In addition, the results of fluorescence, synchronous fluorescence and CD suggest that the conformation of HSA was not changed obviously on the binding of nevadensin. Fluorescence experiment and study of computational modeling indicate that the main interaction is hydrophobic force and there are also hydrogen bonds

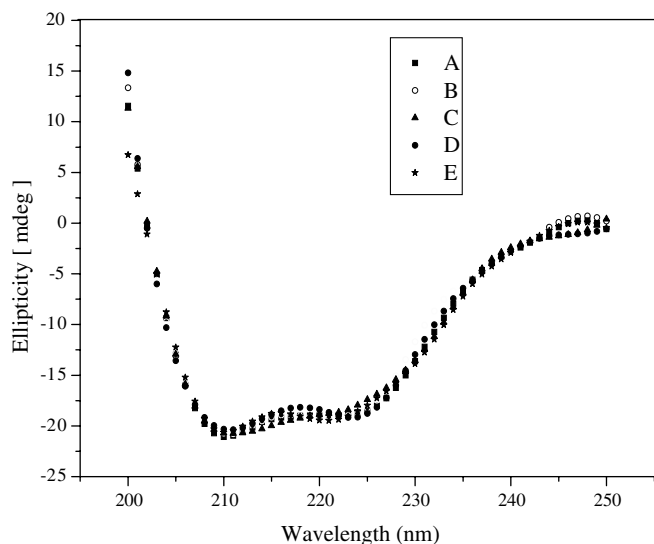


Fig. 8. The CD spectra of the HSA–nevadensin system in Tris buffer solution of pH 7.40 at 296 K. HSA concentration was kept fixed at 1.5 μ M (A); in HSA–nevadensin system, the nevadensin concentration was 0.5 μ M (B), 1.5 μ M (C), 6 μ M (D), 12 μ M (E).

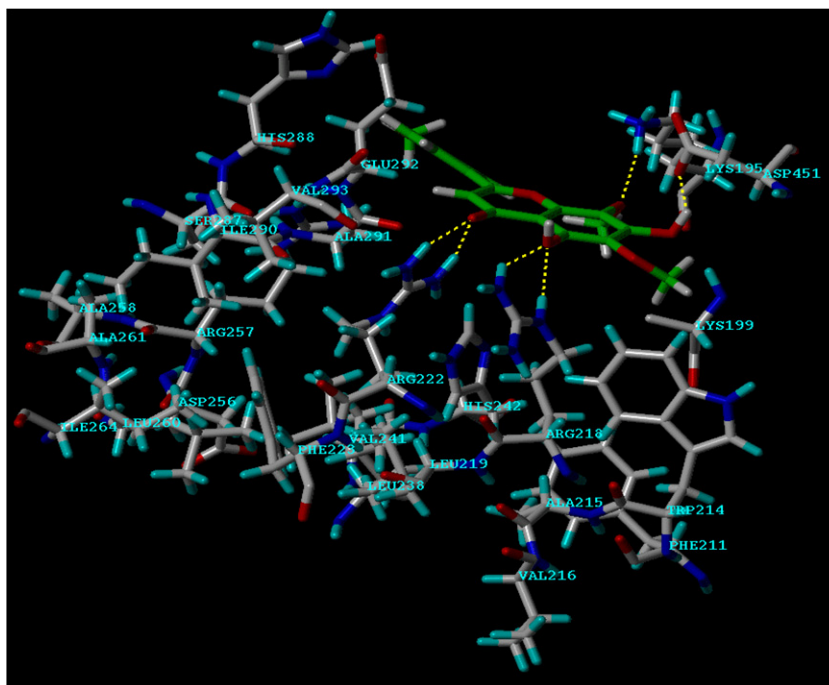


Fig. 9. Interaction mode between nevadensin and HSA, only residues around 6.5 \AA of the ligand are displayed. The residues of HSA and the ligand structure are all represented using stick model. The hydrogen bond between the ligand and the protein is represented using yellow dashed line.

between nevadensin and Arg-218, Arg-222, Lys-195, and Asp-451 residues of HSA.

The binding study of drugs to proteins is greatly important in pharmacy, pharmacology and biochemistry and so on. This study can provide important insight into the interactions of the physiologically important HSA with drugs. Besides, useful information can be also obtained about the effect of environment on the structure features of HSA which may be correlated to its physiologically activity.

References

- [1] D.C. Carter, J.X. Ho, *Adv. Protein Chem.* 45 (1994) 153.
- [2] S. Rusznyak, A. Szent-Gyorgyi, *Nature* 138 (1936) 27.
- [3] S.W. Lamson, M.S. Brignall, *Altern. Med. Rev.* 5 (2000) 196.
- [4] D.K.F. Meijer, P. Van der sluijs, *Pharm. Res.* 6 (1989) 105.
- [5] S. Sugio, A. Kashima, S. Mochizuki, M. Noda, K. Kobayashi, *Protein Eng.* 12 (1999) 439.
- [6] S. Bi, L. Ding, Y. Tian, D. Song, X. Zhou, X. Liu, H. Zhang, *J. Mol. Struct.* 703 (2004) 37.
- [7] W.Y. He, Y. Li, C.X. Xue, Z.D. Hu, X.G. Chen, F.L. Sheng, *Bioorg. Med. Chem.* 13 (2005) 1837.
- [8] C. Dufour, O. Dangles, *Biochim. Biophys. Acta* 1721 (2005) 164.
- [9] Y. Li, W. He, Y. Dong, F. Sheng, Z. Hu, *Bioorg. Med. Chem.* 14 (2006) 431.
- [10] J. Tang, W. Wang, F. Luan, X. Chen, *Int. J. Biol. Macromol.* 37 (2005) 85.
- [11] M.X. Xie, X.Y. Xu, Y.D. Wang, *Biochim. Biophys. Acta* 1724 (2005) 215.
- [12] C.D. Kanakis, P.A. Tarantilis, M.G. Polissiou, S. Diamantoglou, H.A. Tajmir-Riahi, *J. Mol. Struct.* 798 (2006) 69.
- [13] M.X. Xie, M. Long, Y. Liu, C. Qin, Y. Wang, *Biochim. Biophys. Acta* 1760 (2006) 1184.
- [14] T.K. Maiti, K.S. Ghosh, S. Dasgupta, *Proteins: Structure, Function, and Bioinformatics* 64 (2006) 355.
- [15] F. Zsila, Z. Bikadi, M. Simonyi, *Biochem. Pharmacol.* 65 (2003) 447.
- [16] B. Sengupta, P.K. Sengupta, *Biochem. Biophys. Res. Commun.* 299 (2002) 400.
- [17] B. Sengupta, A. Banerjee, P.K. Sengupta, *J. Photochem. Photobiol. B* 80 (2005) 79.
- [18] Y. Xu, Zhong Yao Zhi, vol. 4, The People's Medical Publishing House, Beijing, 1988, p. 351.
- [19] Y. Liu, H. Wagner, R. Bauer, *Phytochemistry* 48 (1998) 339.
- [20] SYBYL Software, Version 6.9, St. Louis, Tripos Associates Inc. 2002.
- [21] A. Sulkowska, *J. Mol. Struct.* 614 (2002) 227.
- [22] T.G. Dewey (Ed.), *Biophysical and Biochemical Aspects of Fluorescence Spectroscopy*, Plenum Press, New York, 1991, pp. 1–41.
- [23] W.R. Ware, *J. Phys. Chem.* 66 (1962) 455.
- [24] S.S. Lehrer, *Biochemistry* 10 (1971) 3254.
- [25] J.N. Tian, J. Liu, Z.D. Hu, X.G. Chen, *Bioorg. Med. Chem.* 13 (2005) 4124.
- [26] M.H. Rahman, T. Maruyama, T. Okada, K. Yamasaki, M. Otagiri, *Biochem. Pharmacol.* 46 (1993) 1721.
- [27] P.D. Ross, S. Subramanian, *Biochemistry* 20 (1981) 3096.
- [28] J.R. Lakowicz, *Principles of Fluorescence Spectroscopy*, second ed., Plenum Press, New York, 1999, p. 13.
- [29] M. Yang, P. Yang, X. Xi, *Chin. Sci. Bull.* 42 (1997) 1276, in Chinese.
- [30] J.N. Tang, S.D. Qi, X.G. Chen, *J. Mol. Struct.* 779 (2005) 87.
- [31] L. Cyril, J.K. Earl, W.M. Sperry, *Biochemists Handbook*, E & FN Epon Led. Press, London, 1961, p. 83.
- [32] J.S. Johansson, *J. Biol. Chem.* 272 (1997) 17961.
- [33] E.A. Brustein, N.S. Vedenkina, M.N. Irkova, *Photochem. Photobiol.* 18 (1973) 263.
- [34] J.N. Miller, *Proc. Anal. Div. Chem. Soc.* 16 (1979) 203.
- [35] P. Yang, F. Gao, *The Principle of Bioinorganic Chemistry*, Science Press, Beijing, 2002, p. 349.
- [36] A. Papadopoulou, R.J. Green, R.J. Frazier, *J. Agric. Food. Chem.* 53 (2005) 158.
- [37] L. Shang, X. Jiang, S.J. Dong, *J. Photochem. Photobiol. A* 184 (2006) 93.
- [38] C. Simon, K. Barathieu, M. Laguerre, J.M. Schmitter, E. Fouquet, I. Pianet, E.J. Dufourc, *Biochemistry* 42 (2003) 10385.
- [39] X.M. He, D.C. Carter, *Nature* 358 (1992) 209.